#### Please cite the Published Version

Yaylali, Banu, Gulten, Gokhan, Yesilyurt, Mustafa, Totik, Yasar, Kulczyk-Malecka, Justyna , Kelly, Peter and Efeoglu, Ihsan (2025) Analysis of four-point bending test for Nb, Ta, and V-doped CrYN thin films deposited by closed-field unbalanced magnetron sputtering. Surface and Coatings Technology, 518. 132903 ISSN 0257-8972

**DOI:** https://doi.org/10.1016/j.surfcoat.2025.132903

Publisher: Elsevier

Version: Accepted Version

Downloaded from: https://e-space.mmu.ac.uk/642793/

Usage rights: Creative Commons: Attribution 4.0

**Additional Information:** This is an author accepted manuscript of an article published in Surface and Coatings Technology, by Elsevier. This version is deposited with a Creative Commons Attribution 4.0 licence [https://creativecommons.org/licenses/by/4.0/], in accordance with Man Met's Research Publications Policy. The version of record can be found on the publisher's website.

Data Access Statement: Data will be made available on request.

#### **Enquiries:**

If you have questions about this document, contact openresearch@mmu.ac.uk. Please include the URL of the record in e-space. If you believe that your, or a third party's rights have been compromised through this document please see our Take Down policy (available from https://www.mmu.ac.uk/library/using-the-library/policies-and-guidelines)

# Analysis of Four-Point Bending Test for Nb, Ta, and V-Doped CrYN Thin Films **Deposited by Closed-Field Unbalanced Magnetron Sputtering**

Banu Yaylali<sup>1</sup>, Gokhan Gulten<sup>1</sup>, Mustafa Yesilyurt<sup>1</sup> Yasar Totik<sup>1</sup>, Justyna Kulczyk-Malecka<sup>2</sup>, 4 Peter Kelly<sup>2</sup>, Ihsan Efeoglu<sup>1\*</sup> 5

- <sup>1</sup>Faculty of Engineering, Department of Mechanical Engineering, Atatürk University, 25240 6
- Erzurum, Türkiye 7
- <sup>2</sup> Surface Engineering Group, Manchester Metropolitan University, Manchester M1 5GD, UK 8

#### 9 **Abstract**

1

2 3

- The increasing expectations and requirements for engineering materials are steadily compelling 10 11 researchers to evolve and innovate further. Adding transition metals to coating architectures is becoming increasingly attractive as it improves structural and mechanical properties. In this 12 work, CrYN thin films incorporating transition metals Nb, Ta, and V were deposited on a 316L 13 stainless steel substrate using Closed Field Unbalanced Magnetron Sputtering (CFUBMS) with 14 a DC and Pulsed-DC power supply. The microstructural properties of the thin films were 15 analyzed using scanning electron microscopy (SEM), while X-ray diffraction (XRD) and X-ray 16 photoelectron spectroscopy (XPS) provided a comprehensive understanding of the coating 17 structure by providing information on crystallographic and surface chemical properties. 18 19 Mechanical properties were evaluated using nanoindentation testing, which provided accurate measurements of hardness and elasticity, while scratch testing assessed critical load values. In 20 addition, four-point bending tests were performed at room temperature to characterize the 21 22 CrYN:Nb/Ta/V transition metal nitrides (TMNs), providing a more comprehensive analysis of the mechanical behavior (bending strength and elastic modulus) and adhesion properties of the 23 coating. The mechanisms of coating damage (crack formation and density, spalling, flaking, 24 25 and separated coating particles) were analyzed as a result of four-point bending tests. The 26 Taguchi approach was employed to investigate how deposition parameters—such as target current, duty cycle, and pulse frequency affect elastic modulus and bending strength. Superior 27 structural (homogeneous and dense film) and mechanical properties (CrYN:Nb/Ta/V high 28 hardness values of 21.4, 18.2, 16.1 GPa, and bending strengths of 707, 711, and 709 MPa, 29 respectively) were obtained. The positive correlation between hardness and bending strength 30 points to an enhancement in the overall durability of the thin film.
- **Keywords:** Magnetron sputtering, AISI 316L, CrYN thin films, niobium, tantalum, vanadium 32
- additions, adhesion, and four-point bending tests 33
- 34 Corresponding Author: Ihsan Efeoglu (<u>iefeoglu@atauni.edu.tr</u>)

# 1. Introduction

35

36

37

38

39

40

41

42

43

44

45

46

47

48

49

50

51

52

53

54

55

56

57

58

59

60

61

62

63

64

65

Developing and changing technological factors and industry's ever-increasing demand for engineering materials are encouraging researchers to synthesize more and more innovative and functional thin films. Material surfaces operating under aggressive/harsh conditions will inevitably be damaged by degradation under conditions such as high temperature, high pressure, oxidation, corrosion, etc. Coatings applied to the material surface extend the life of the components, reduce costs and support the system to operate in safer conditions. When synthesizing functional thin films, transition metals (Cr, Nb, Ta, Ti, V, Mo, Zr, Y, Al, etc.) are widely preferred due to their superior mechanical, tribological and electrochemical contributions to the structure. Chrome nitride coatings show high hardness, fine-grained internal structure, oxidation and corrosion resistance [1-5]. The effects of Nb (Niobium) doping in nitride-based films have been examined and it has been observed that it leads to the formation of a dense, homogeneous and finer grained microstructure, resulting in an increase in mechanical properties and corrosion resistance [6,7-9]. In a study by Hovsepian et al., elements such as Cr and Nb were doped into the structure and high hardness, good wear, and corrosion resistance were attributed to the Me-nitrides formed in the structure [10]. Other studies have synthesized Nb-doped chromium nitride thin films and observed positive changes in hardness, elastic modulus and plastic deformation resistance [11,12]. Similarly, the beneficial effects of tantalum (Ta) additives on corrosion/oxidation resistance, mechanical properties and thermal stability are known from the literature [13-16]. Rapoport et al. found that the addition of V (Vanadium) to nitride-based films will reduce the friction coefficient of the film and increase its wear performance, i.e. improve its tribological properties [17]. In our previous studies, mechanical, tribological and electrochemical properties of Nb, Ta and V doped films were investigated in detail using Taguchi design of experiments method. In this study, structural and mechanical properties were examined by focusing on three samples (MC-1, MC-2, and MC-3) selected in the light of the findings obtained in our previous studies for Nb, Ta, and V-doped films. The selected samples are those that exhibited the highest hardness values in our previous studies. Moreover, these selected coatings also exhibited the highest bending strength. As expected, these two mechanical tests corroborated each other. Based on the data obtained, our study was designed around these three samples [18,19].

# 2. Materials and methods

- The preferred substrate for the synthesized CrYN:Nb/Ta/V films was 316L stainless steel (SS).
- Using 400, 600, 800, 1000, and 1200 mesh SiC abrasives, respectively, the substrates were

polished from coarse to fine grain, decreasing the surface roughness to a value Ra  $\approx 0.02 \mu m$ . To improve adhesion to the coating and passivate the surface, they were cleaned with acetone and ethyl alcohol in an ultrasonic bath for 30 minutes prior to the procedure. After that, the substrates were etched in a V2A Etchant solution, which contained 10 ml of nitric acid, 100 ml of distilled water, and 100 ml of HCl. In order to produce CrYN:Nb/Ta/V films, the process employed two (99.95%) CrY targets (atomic percent Cr 97%, Y 3%), one (99.95%) niobium/tantalum target, or one (99.95%) vanadium target. The CFUBMS (Closed Field Unbalanced Magnetron Sputtering) technique, which can operate in DC or Pulsed DC mode, was used to carry out the coating procedure. Ar gas (99.99%) was utilized for target sputtering and plasma production, whereas N<sub>2</sub> gas (99.99%) was utilized as the reactive gas. Before the deposition process, the substrate was cleaned with Ar + ions for 30 minutes at 800 V bias voltage to improve adhesion between the substrate and the coating and to get away of impurities. The deposition process was optimized employing a Taguchi L9 orthogonal array to systematically evaluate the effects of key sputtering parameters-namely, CrY target current, deposition pressure, and the duty cycle of the pulsed-DC power supplied to the CrY targets. These parameters were deliberately chosen as control factors due to their pronounced impact on the coating growth dynamics: (a) the CrY target current governs the sputtering rate of Cr and Y atoms, thereby influencing the resulting film thickness, chemical composition, and microstructural characteristics; (b) the deposition pressure affects the mean free path and kinetic energy of the sputtered species, consequently altering adatom mobility, nucleation mechanisms, and coating density; and (c) the duty cycle, defined as the fraction of each pulse period during which power is delivered to the CrY targets in pulsed-DC mode, dictates ionization behavior, thermal input to the target, and plasma-substrate interactions, which collectively influence residual stress, grain refinement, and defect concentration within the coating [18,19]. The experimental parameters of the coating process are given in Table 1. Target current (1, 1.5, and 2 A), deposition pressure (0.15, 0.25, and 0.35 Pa), pulse frequency (100 kHz), and duty cycle (50–70–85%) were the deposition parameters examined in the array. The synthesis procedure made use of DC power (Nb, Ta, and V target) and Pulsed-DC (CrY target) supplies. A Pulsed-DC power supply was employed for the CrY target in order to stabilize the reactive sputtering process and enhance coating quality. In reactive atmospheres containing nitrogen, continuous DC sputtering often leads to target poisoning, charge accumulation, and arcing, which can cause plasma instability and surface defects. The pulsed-DC configuration mitigates these problems by periodically reversing the target potential, thereby allowing charge neutralization and preventing arc formation. This approach provides

68

69

70

71

72

73

74

75

76

77

78

79

80

81

82

83

84

85

86

87

88

89

90

91

92

93

94

95

96

97

98

99

100

more stable plasma conditions, improved control of the reactive gas phase, and enhanced ion energy uniformity. Consequently, pulsed-DC sputtering promotes denser film growth, reduced residual stress, and improved adhesion between the coating and substrate compared to conventional DC sputtering. Figure 1 graphically depicts the architecture of the stored microstructure as well as a model of the Teer Coating Ltd.-patented (UDP550) CFUBMS system. Using a Rigaku 2000 D max diffractometer, X-ray diffraction (XRD) was carried out with a Cu-Kα radiation source spanning the range between 20° and 100° 2 theta and 2°/min scan rate. The coatings' microstructure and surface morphology were examined using a Zeiss Sigma 300 scanning electron microscope (SEM), and elemental analysis was conducted using an XPS (X-ray Photoelectron Spectroscopy) and energy dispersive spectroscopy (EDS) equipment. A nanoindentation tester made by Anton Paar was used to analyze the thin films' nanohardness. By applying a Berkovich indenter, a maximum load of 3.00 mN and a loading rate of 6.00 mN/min were applied for 10 s. The critical load values of the thin film samples were determined at three different points on each sample using a CSM Instruments scratch tester with an increasing loading rate of 100 N/min and a Rockwell-C type diamond indenter with a tip radius of 200 µm. 4-point bending tests were performed on a Zwick/Roell Z250 bending machine (Fig. 2). Preload 5 N, test speed: It was set as 5 mm/min. The support span was designed to be twice the loading span. The damage mechanisms of Nb/Ta/V-doped CrYN thin films were investigated by visualizing their optical images from the outer bending surfaces (Fig. 13).

**Table 1.** Deposition Parameters and Taguchi Experimental Design [18,19]

The variable Parameters CrY Target Current (A) Deposition Pressure (Pa)	Level 1	Level 2	Level 3
	1	1.5	2
	0.15	0.25	0.35
Duty Cycle (%)	50	70	85

The Constant Parameters	
CrY Interlayer	CrY: 2A (10 min)
CrY (Nb, Ta, V)N	Nb/Ta/V: 2A, (90 min)
N <sub>2</sub> Flow Rate (sccm)	6
Pulse Frequency (kHz)	100

	<b>Duty Cycle</b>	<b>Deposition Pressure</b>	CrY Target		
	(%)	(Pa)	Current (A)		
MC-1	50	0.15	1		
MC-2	70	0.25	1.5		
MC-3	85	0.35	2		

102

103

104

105

106

107

108

109

110

111

112

113

114

115

116

117

118

119

120

121

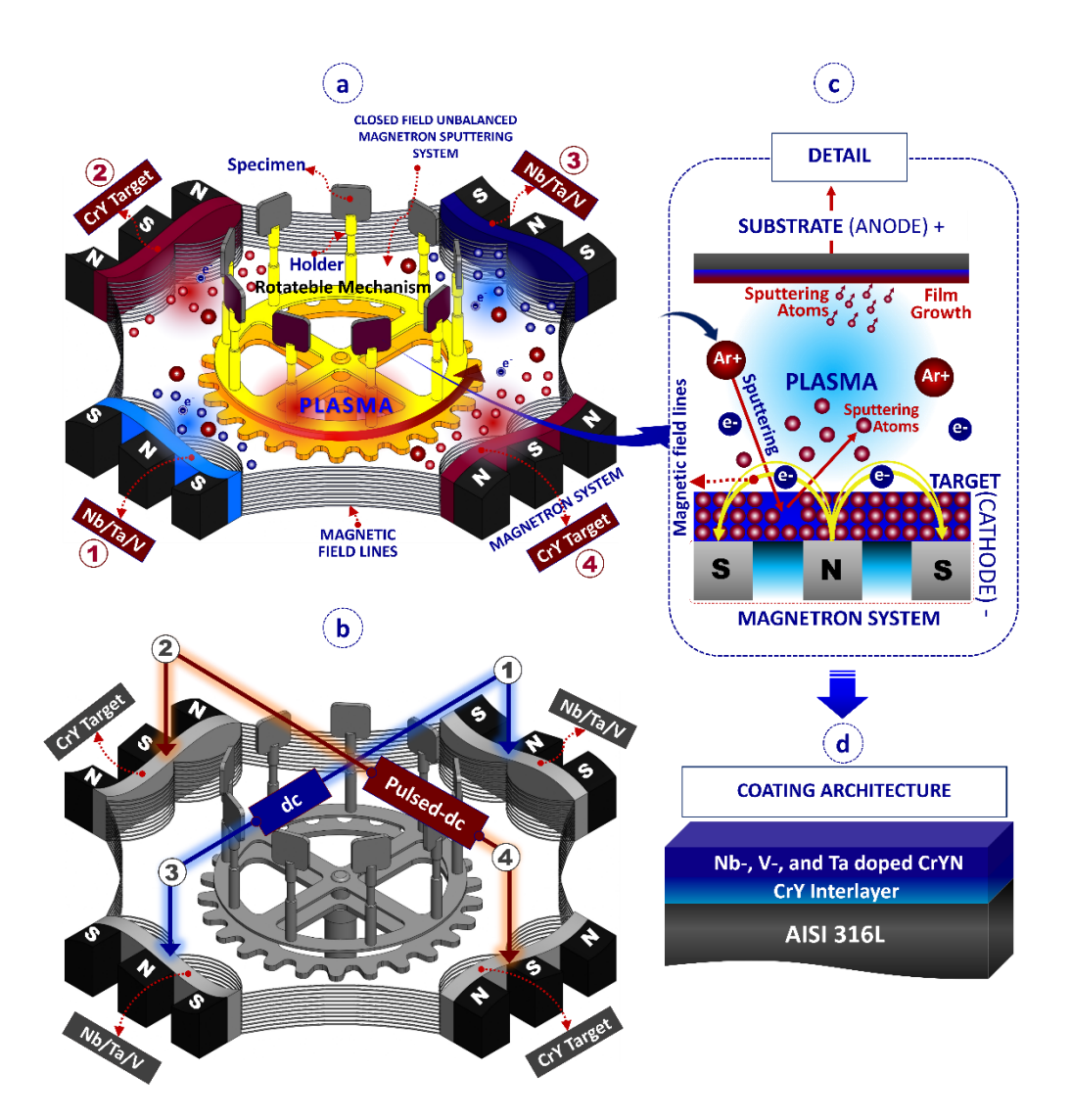


Fig. 1 a, b) The target magnetron and the power supplies configuration of the CFUBMS deposition system c) sputtering detail and d) structural design of Nb-, Ta, and V-doped CrYN coatings detail

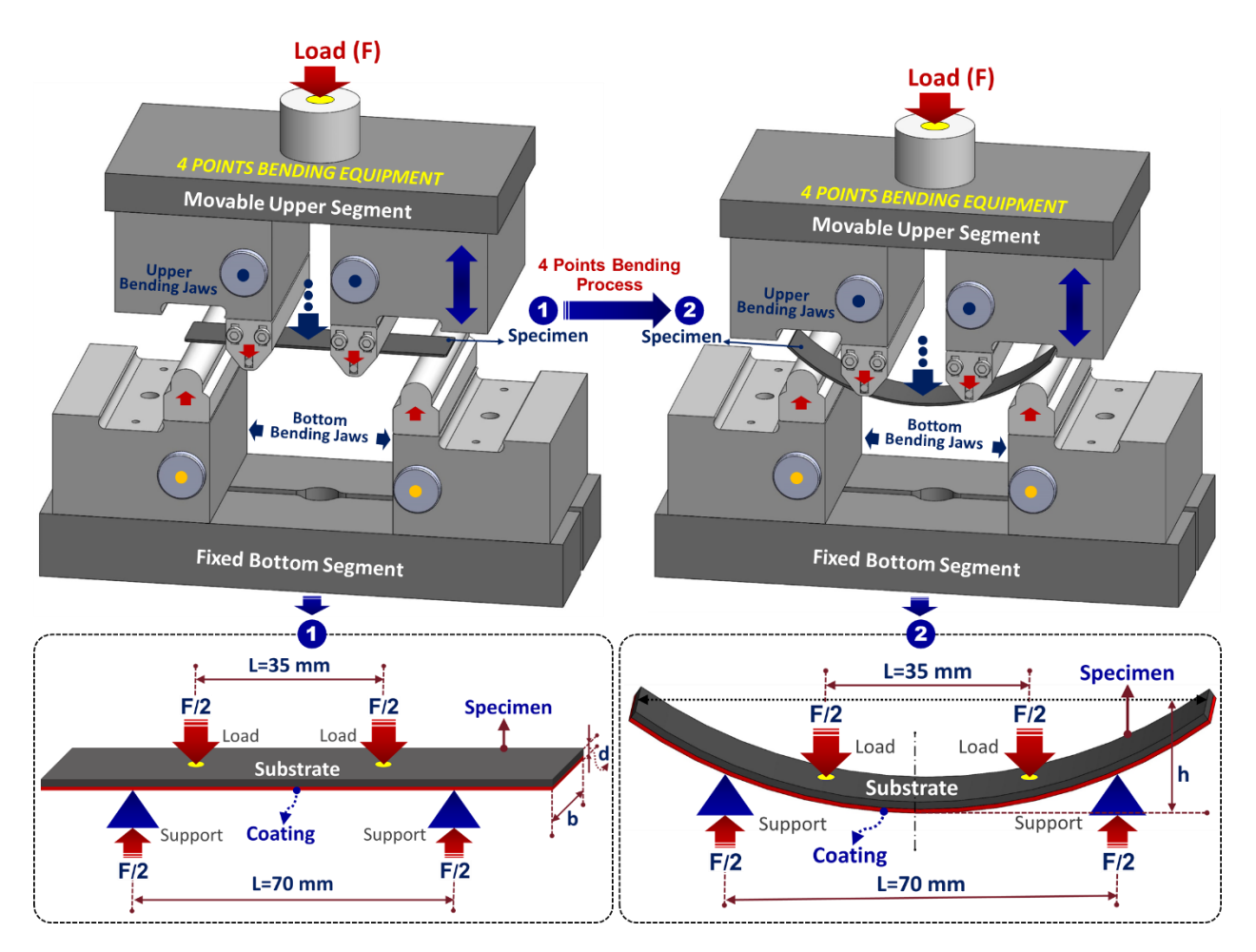


Fig. 2. 4 Schematic Representation of the Point Bending Equipment and experimental design

# 3. Results and discussions

Using the various array variables, XRD analysis of the Nb/Ta/V doped thin films deposited onto 316L stainless steel is shown in Fig. 3. Examining the thin films reveals strongly cubic CrN and Cr<sub>2</sub>N peaks in addition to the primary peaks from the substrate. NbN and Tadoped TaN peaks are seen in the niobium/tantalum-doped thin film, respectively (Fig. 3a and b). The literature has established that the (111) orientation found in nitride films containing transition metals has an impact on the structure's hardness [20]. Furthermore, it has been suggested in the literature that yttrium is present in the crystal structure as a chromium substitution atom; in this regard, XRD peak analysis suggests that yttrium is present in the structure as a chromium substituent atom [21-24]. Both chromium and yttrium have 3 valence electrons. The peak with  $Cr_2N$  phase showed a shift in angles to the right (Fig. 3a, b and c). This change is explained by the expansion of the chromium cages by yttrium, which has a large atomic radius [24].

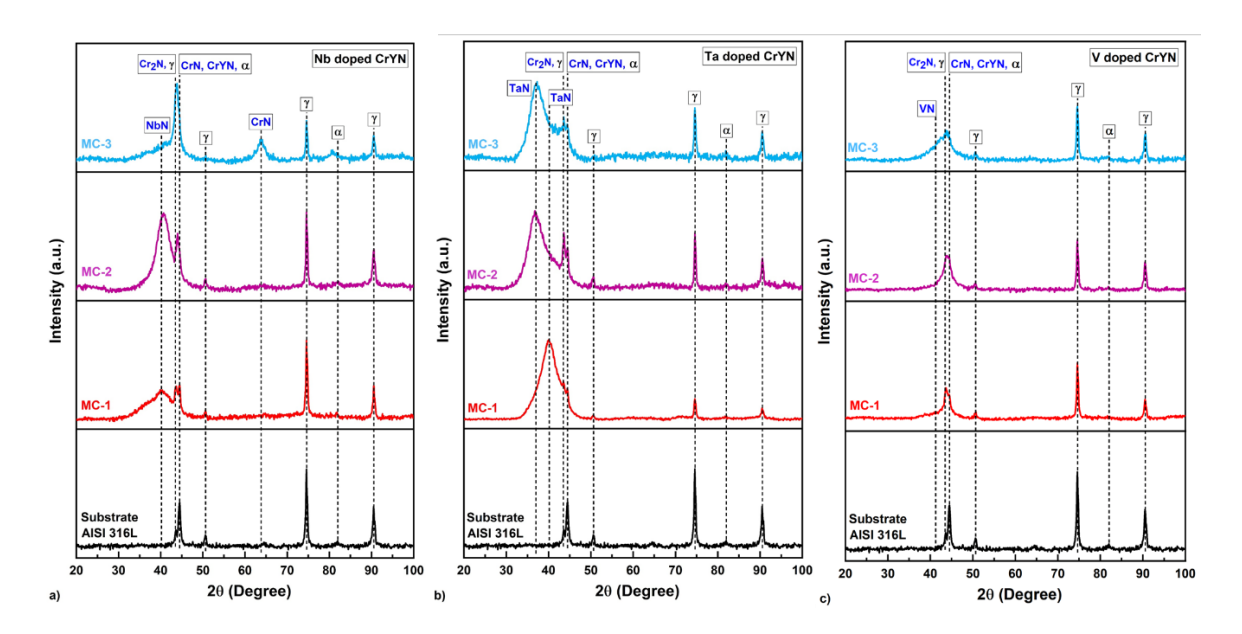


Fig. 3. XRD graph of CrYN thin films; a) Nb-doped and b) Ta-doped c) V-doped [18, 19]

145

146

147

148

149

150

151

152

153

154

155

156

157

158

159

160

161

162

A method for determining a material's mechanical characteristics at the nanoscale, particularly its hardness and elastic modulus, is called nano-hardness, or nanoindentation. It entails using a sharp indenter (Berkovich indenter) to apply a controlled force to a material's surface and measuring the depth of indentation. The mechanical characteristics of thin films can be examined using this sensitive method. For Nb, Ta and V-doped thin films, the maximum indentation depth was required to be less than 100 nm. The indentation depth was maintained below 10% of the coating thickness to minimize substrate influence, while acknowledging that surface roughness may still affect the measured hardness, particularly at lower indentation loads. When the nanohardness values of niobium, tantalum and vanadium doped CrYN films were investigated, it was observed that the highest hardness values were 21.4 GPa, 18.2 GPa and 16.1 GPa, respectively. This trend can be attributed to the differing effects of each dopant on film microstructure. Nb addition promotes grain refinement and solid-solution strengthening, leading to a denser microstructure and higher resistance to localized deformation. Ta incorporation provides intermediate hardening, while V doping, although slightly reducing hardness, enhances film adhesion and toughness, as supported by the scratch and bending test results. Typical nanoindentation load-depth curves and nanohardness results for CrYN:Nb/Ta/V thin films are given in Fig. 4.

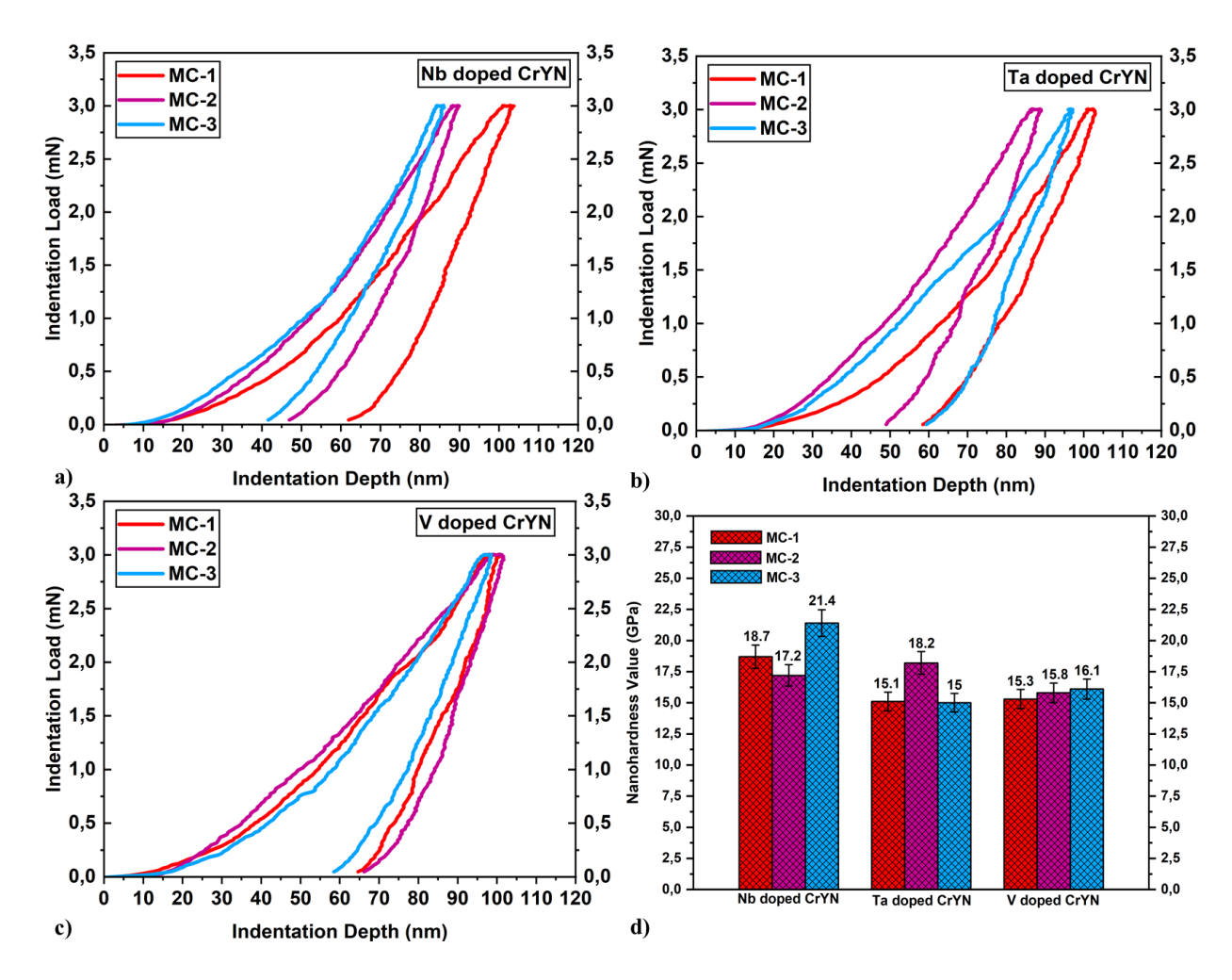


**Fig. 4.** a) Nanoindentation curves of Nb-doped CrYN thin films, b) Nanoindentation curves of Ta-doped CrYN thin films, c) Nanoindentation curves of V-doped CrYN thin films, and d) Hardness values of Nb, Ta and V-doped thin films [18, 19]

The chemical composition of the CrYN:Nb/Ta/V thin films was ascertained by XPS. The resultant spectra show the binding energies of photoelectrons, and XPS gives information about the chemical states and binding energies of the elements in the final structure. Changes in binding energies signify modifications to the structure's chemical and physical characteristics. Figure 5 shows the Gaussian plot of the cumulative curves of the XPS spectra of chromium (Cr2p), yttrium (Y3d), nitrogen (N1s), and niobium (Nb3d) for the CrYN:Nb thin films. The graphs show the peaks for Cr2p3/2, Y3d5/2, Nb3d5/2, and N1s (Fig. 5a). The peaks' respective binding energies were found to be  $570 \pm 2$ ,  $150 \pm 6$ ,  $200 \pm 3$ , and  $393 \pm 3$  eV. In Fig. 5c, the binding energies of Cr2p3/2, Y3d5/2, V2p3/2, and N1s were identified as  $570.5 \pm 4$ ,  $150 \pm 8$ ,  $509 \pm 4$ , and  $393 \pm 4$  eV, respectively.

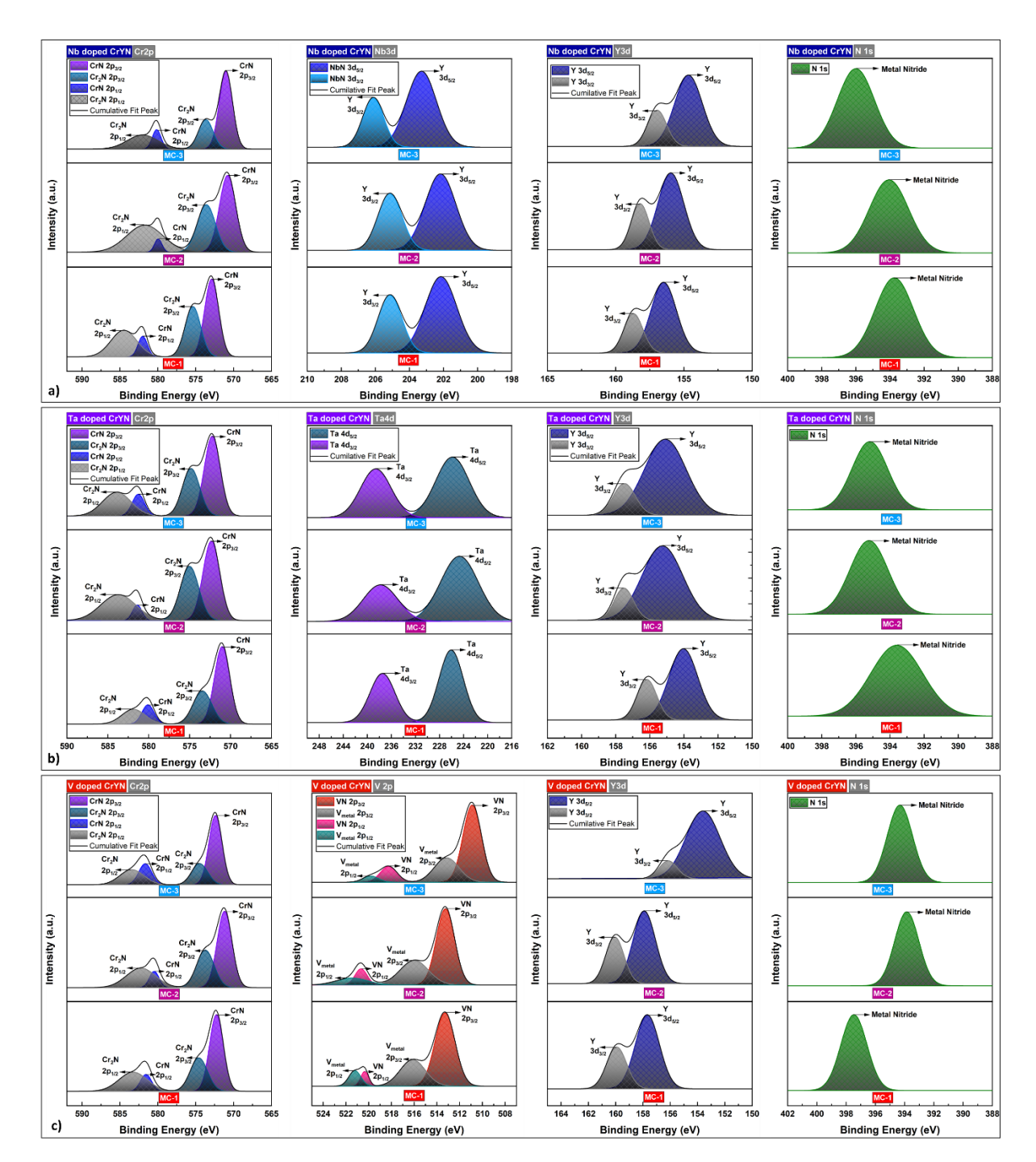


**Fig. 5.** CrYN:Nb/Ta/V thin films, a) Chromium (Cr2p), b) Yttrium (Y3d), c) Niobium (Nb3d), Tantalum (Ta4d), Vanadium (V2p) d) Nitrogen (Nb1s) XPS spectra [18, 19]

The thickness and surface morphological characteristics of the nitride-based coatings were

examined using cross-sectional micrographs of films produced on Si (111) substrates (Fig. 6). As can be seen, dense and uniform structures were seen in both situations. The CrY interlayer is discovered to be around 100 nm. Figure 6 shows that the thickness values of niobium-tantalum and vanadium doped films are MC-1,  $1.32-1.51-1.23~\mu m$ , MC-2,  $1.21-1.83-1.19~\mu m$  and MC-3,  $2.80-2.26-1.86~\mu m$ , respectively.

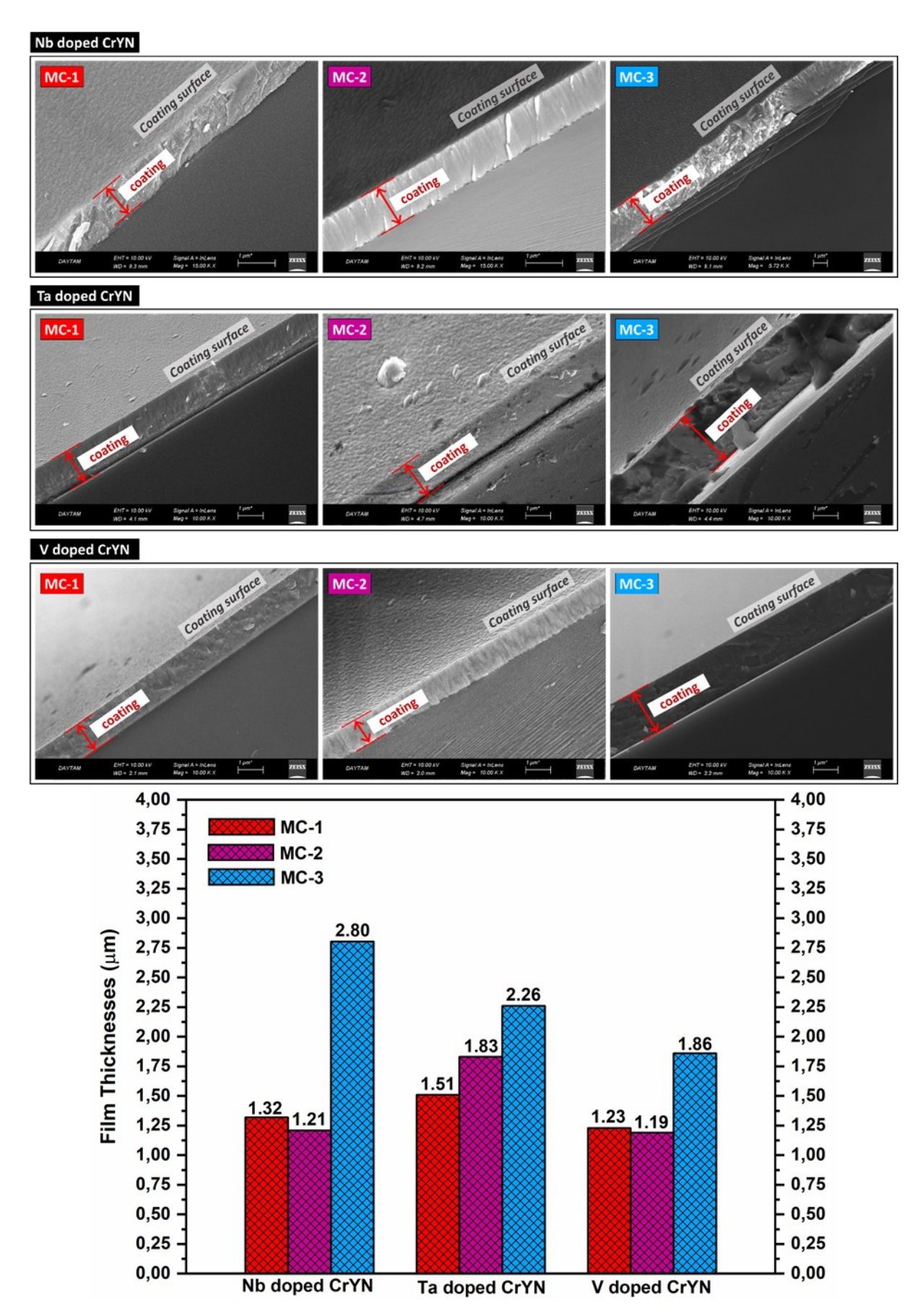


**Fig. 6.** SEM images and film thicknesses of CrYN:Nb/Ta/V doped films MC-1, MC-2, and MC-3 [18, 19].

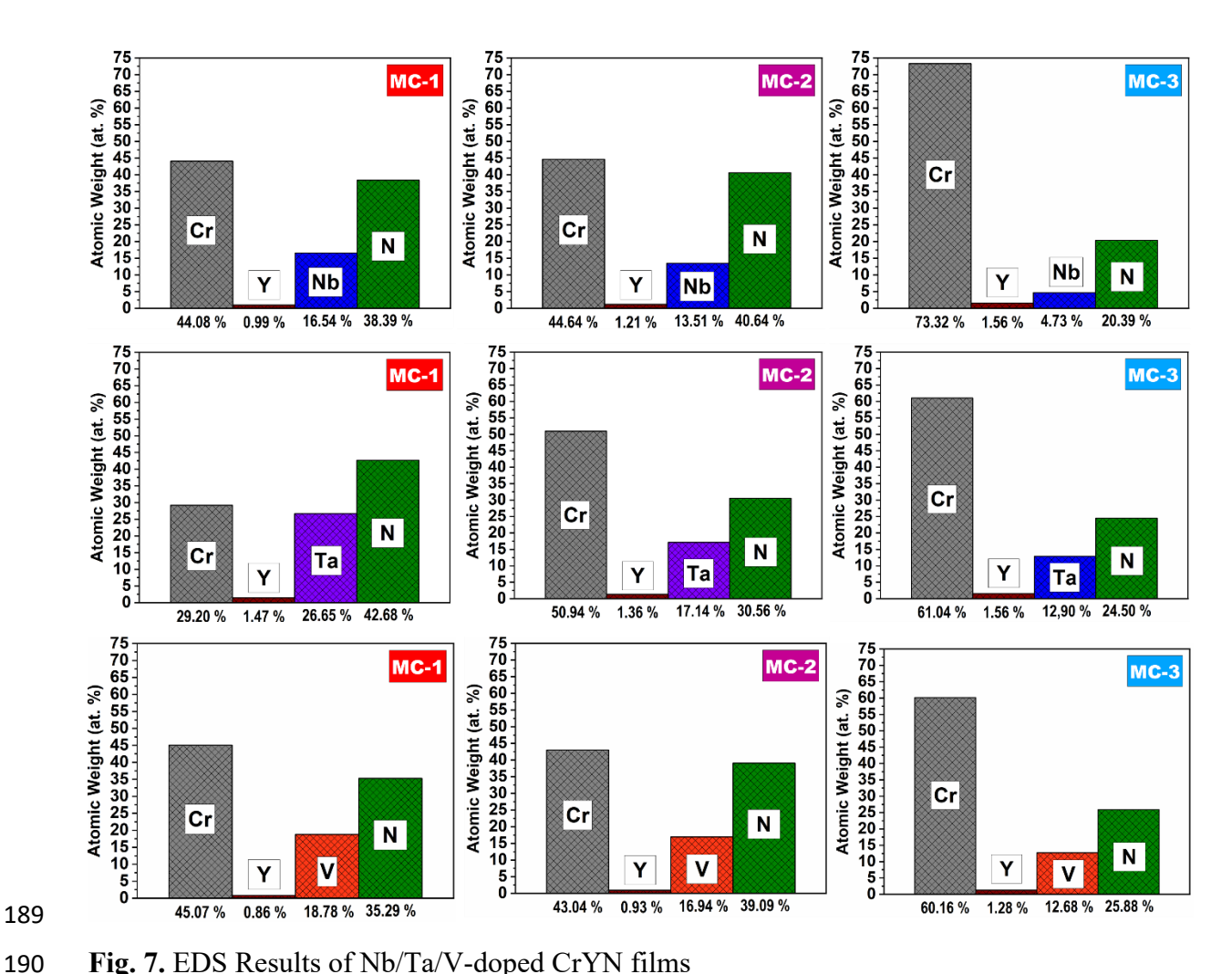


Fig. 7. EDS Results of Nb/Ta/V-doped CrYN films

192

193

194

195

196

197

198

199

200

201

202

EDS results of Nb/Ta/V doped coatings are given in Figure 7. CrYN: The chemical content of the Nb doped film varied from 73.33% to 44.08% of Cr, 1.56% to 0.99% of Y (yttrium), 40.64% to 20.39% of N and 16.54% to 4.73% of Nb. Analyzing the chemical content of CrYN:Ta doped films, it was observed that Cr amounts ranged from 61.04% to 29.2%, Y (yttrium) amounts ranged from 1.56% to 1.36%, N amounts ranged from 42.68% to 24.5% and Ta amounts ranged from 26.65% to 12.9%. When the CrYN:V doped films were evaluated, it was found that the amounts of Cr ranged from 60.16% to 43.04%, the amounts of Y (yttrium) ranged from 1.28% to 0.86%, the amounts of N ranged from 39.09% to 25.88% and the amounts of V ranged from 18.78% to 12.68%.

The scratch test images of Nb/Ta/V-Doped CrYN all films are examined in detail at 30 N, 60 N, 120 N and 150 N shown in Figures 8-10.

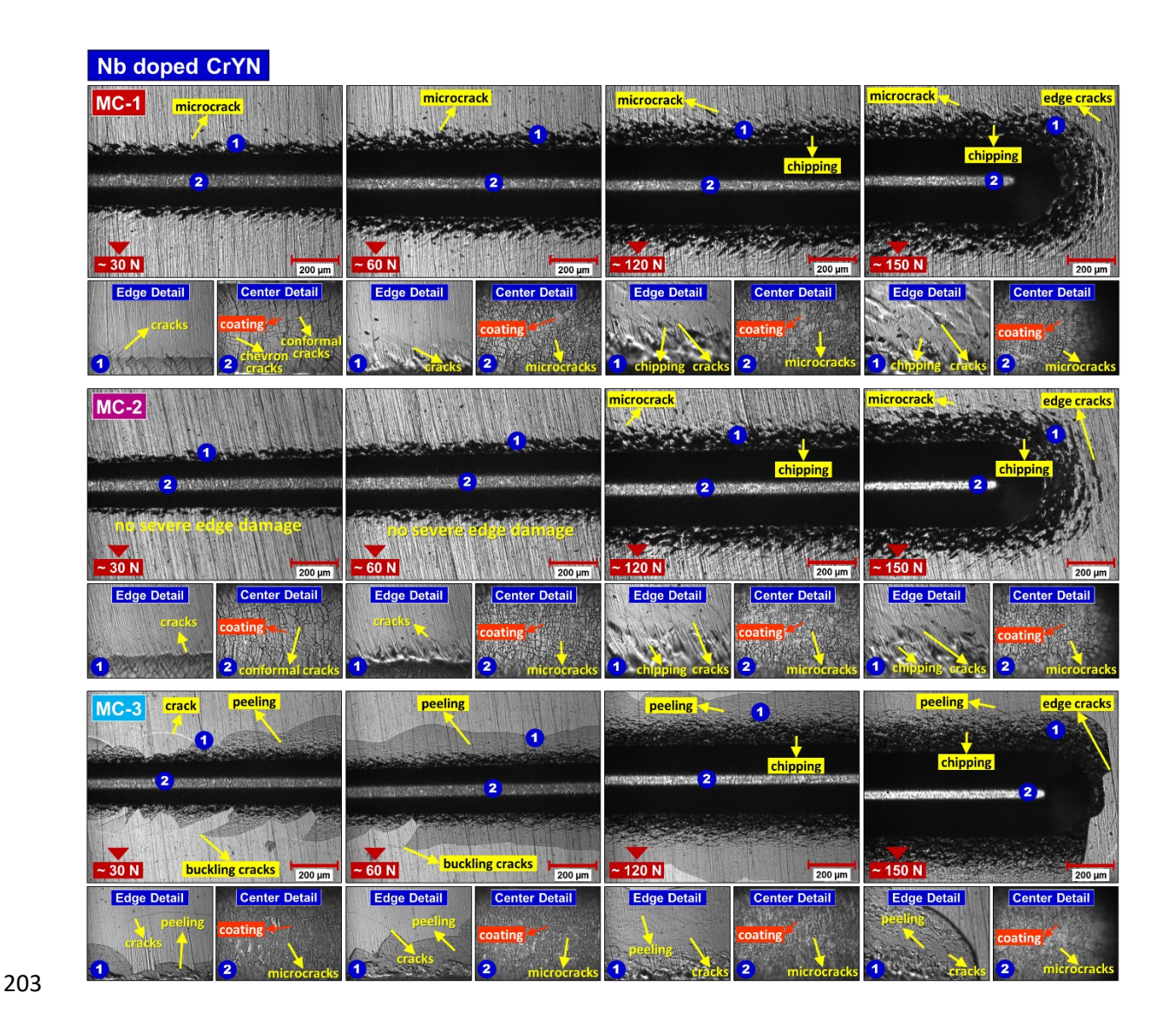


Fig. 8. Scratch Results of Nb-doped CrYN films

Scratch test results of Nb-doped CrYN films showed micro cracks, edge cracks and chipping damage in MC-1. Chevron and conformal cracks were observed in the edge details. MC-2 have micro cracks, edge cracks and chipping damage similar to MC-1. In MC-3, cracks, peelings, chippings and edge cracks were found in the film. For Nb doped films, the most damage occurred in MC-3 film (Fig. 8). This indicates similar results with the results of the four bending tests.

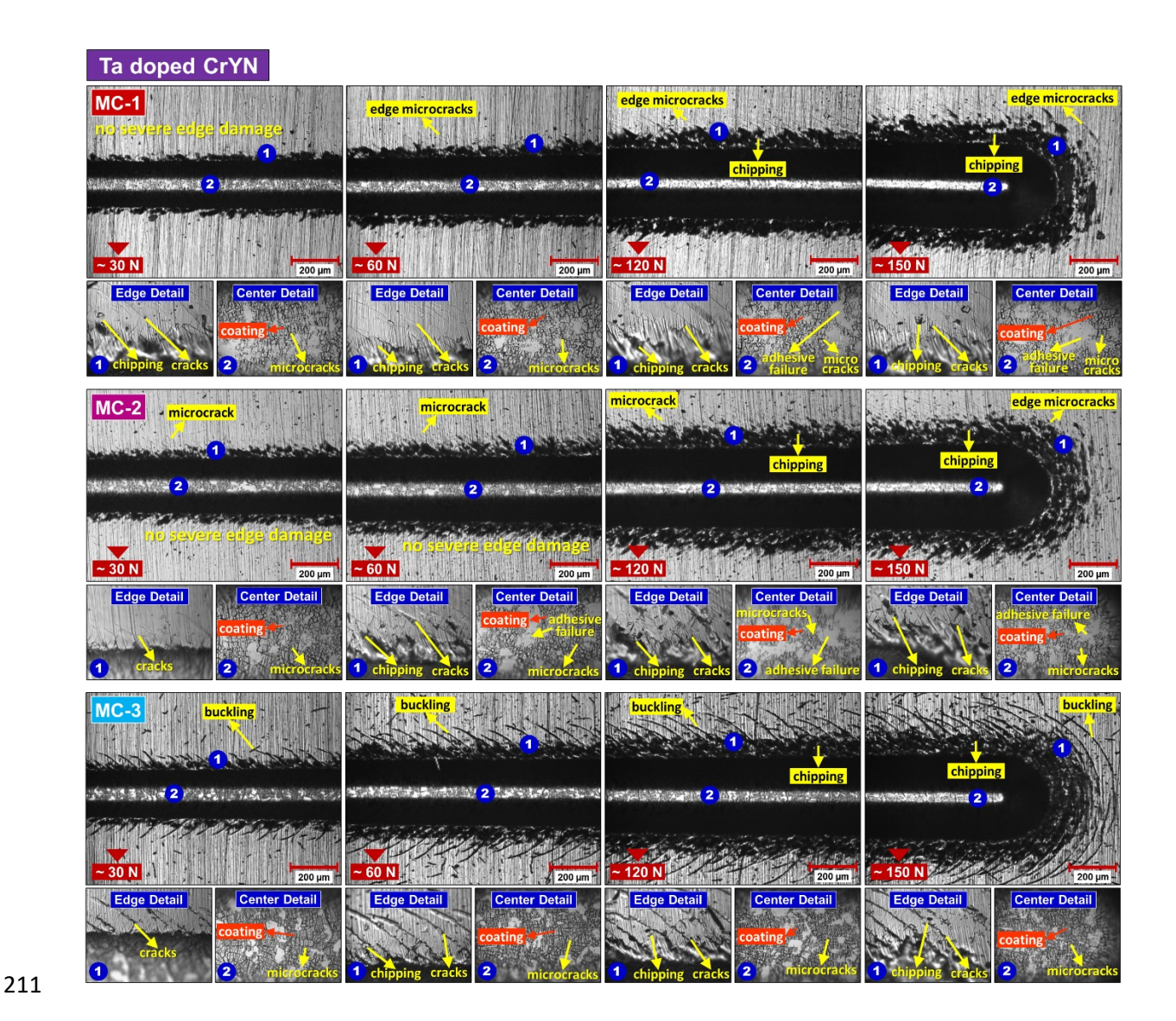


Fig. 9. Scratch Results of Ta-doped CrYN films

The scratch test results for CrYN films containing additives show severe edge damage at 30 N, edge cracks at 60 N, and edge cracks, chipping, and adhesive failure at 120 to 150 N in MC-1. In MC-2, edge cracks at 30 and 60 N, micro cracks and chipping at 120 N, edge cracks and chipping damage were observed at 150 N in addition to the damage at 120 N. In MC-3, cracks and buckling at 30 N, similar damages to 30 N at 60 N and chipping, chipping, buckling and edge cracks at 120 and 150 N were observed. For Ta doped films, the most damage occurred in MC-3 film (Fig. 9). This shows similar results to the results of the four-point bending tests and the two mechanical tests are consistent with each other.

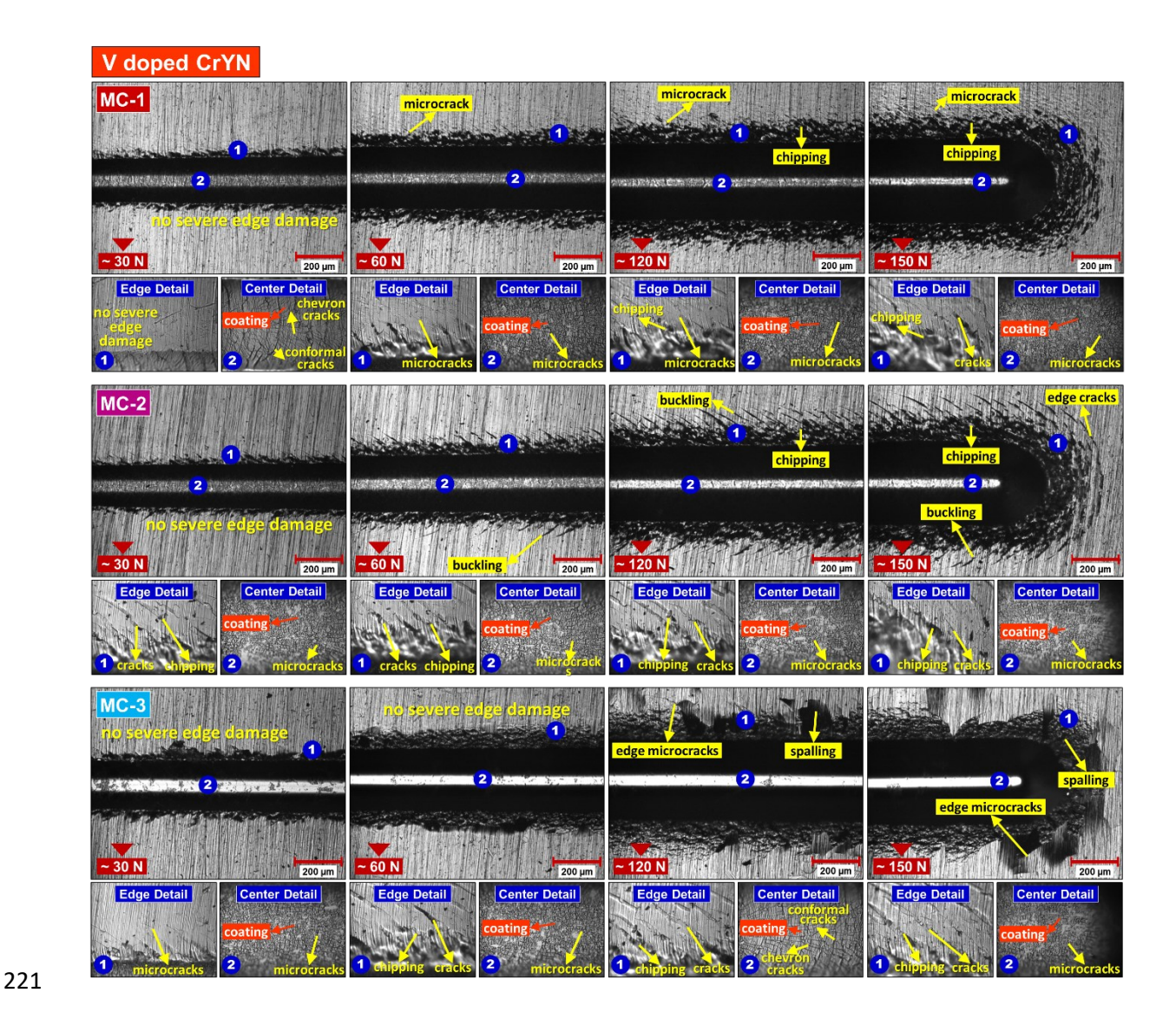
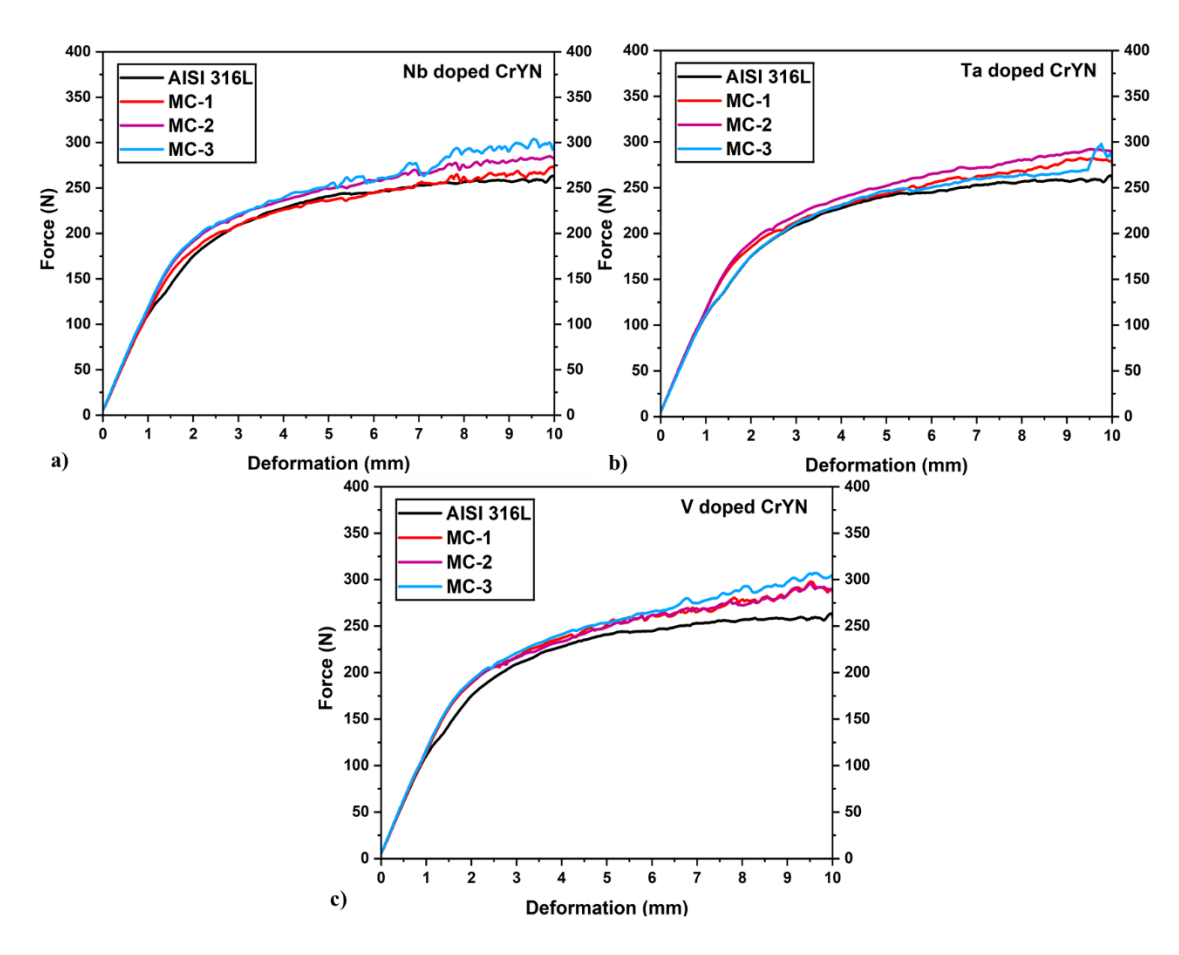


Fig. 10. Scratch Results of V-doped CrYN films

Scratch test results of V-doped CrYN films showed no severe edge damage at 30 N at MC-1, but chevron cracks and conformal cracks were observed in the center details. At 60-120-150 N, micro cracks and chipping damage are present. While no severe edge damage was observed at 30 N in MC-2, edge cracks were observed at 60 N, peeling, chipping and edge cracks were observed at 120 N and 150 N. In MC-3, there was no edge damage at 30 N and 60 N, while micro cracks, conformal cracks, chevron cracks and chipping were observed at 120 and 150 N. For V-doped films, the most damage occurred in MC-3 film (Fig. 10). This shows similar results to the results of the four-point bending test. Again, the results are in agreement with the four-point bending test and the least damage among the three dopants was observed in the vanadium doped films in both tests.

A bending device was used to investigate the mechanical properties of Nb, Ta and V doped chromium yttrium nitride films and the adhesion of the coatings under bending stress. Force (N)-Deformation (mm) graphs were plotted for all experiments (Figure 11a, b and c). Force-Deformation graphs of Nb-doped CrYN films are given in Figure 11a. Fmax (maximum) values of 316L substrate and coatings between MC-1-MC-3 were measured as 257.5 N, 273.5 N, 284.8 N, 303.3 N respectively Fig. 11a. It was found that the deformation amount of Nb-doped films was approximately 10±1 mm. The bending strength results of Nb doped films are given in Figure 12. The Fmax values between MC-1-MC-3 of Ta/V coated films were measured as 282.1 N, 291.7 N, 297 N, (V) 290.6 N 291.9 and 304.3, respectively (Figure 11b, c and Table 2). The graphs of CrYN:Ta thin films are given in Figures 12. All coatings showed higher bending strength compared to the uncoated substrate (Figure 12 and Table 2). Detailed images of the external bending surfaces of CrYN:Nb/Ta/V thin films were taken under optical microscope (Figure 13). Using these images, cracks and their densities, flaking, peeling and separated coating particles in the coating were examined (Figures 14-16).



**Fig. 11.** a) Force-deformation amount graphs of the substrate and CrYN:Nb thin films in the 4-point bending test, b) Force-deformation amount graphs of the substrate and CrYN:Ta thin films in the 4-point bending test, c) Force-deformation amount graphs of the substrate and CrYN:V thin films in the 4-point bending test.

CrYN doped (Nb/Ta/V)	Fmax (N)	L1 (mm)	L (mm)	Thickness (d), (mm)	Width (b), (mm)	Bending moment (Me), (Nmm)	Bending strength (σe), (MPa)	Modulus of Elasticity (E), (GPa)
316L	257.545	17.5	70	1.23	14.84	2253.5	602.2	173.9
MC-1	273.542	17.5	70	1.20	14.56	2393.4	684.9	183.7
MC-2	284.852	17.5	70	1.23	14.87	2492.4	664.7	180.4
MC-3	303.993	17.5	70	1.23	14.92	2659.9	707.0	190.9
MC-1	282.145	17.5	70	1,22	14,72	2468.7	676.0	181.0
MC-2	291,722	17.5	70	1.23	14.87	2552.5	675.2	181.4
MC-3	297.026	17.5	70	1.23	14.49	2598.9	711.3	185.8
MC-1	290.631	17.5	70	1.22	14.97	2543.0	680.3	178.6
MC-2	291.920	17.5	70	1.23	14.77	2554.3	684.7	180.7
MC-3	304.357	17.5	70	1.23	14.88	2663.1	709.7	180.9



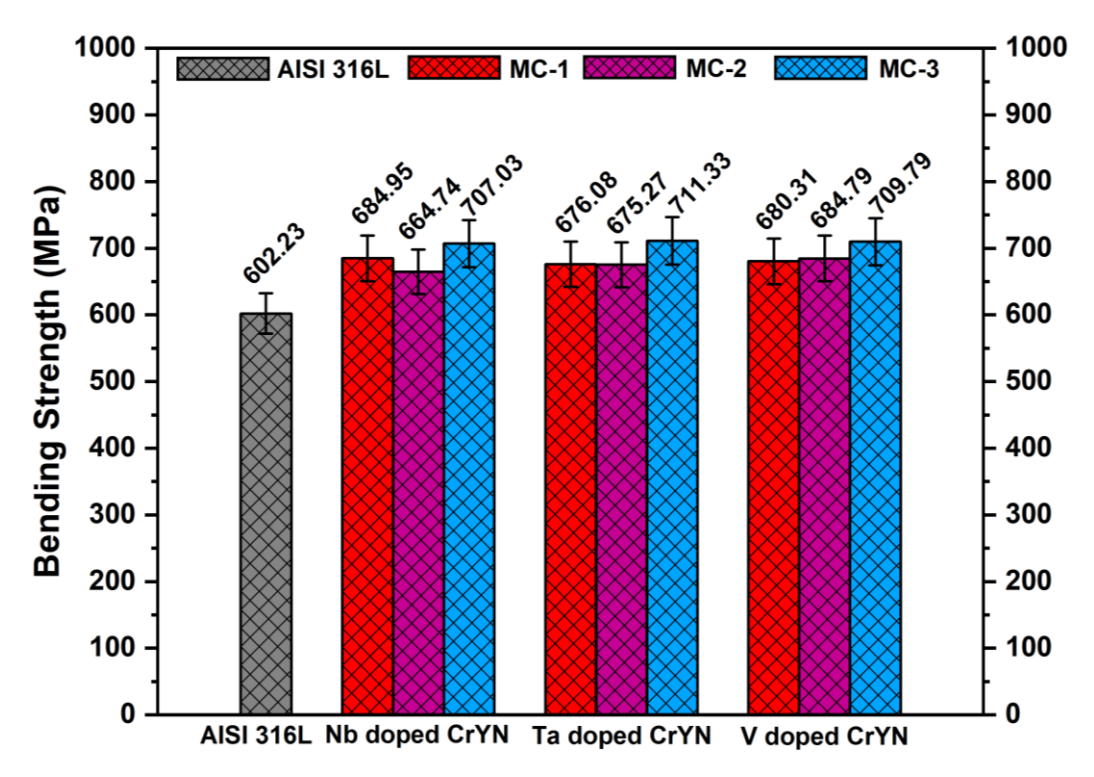


Fig. 12. Bending strength graph of CrYN films doped with Nb, Ta and V.

The bending moment (Me, Nmm) values of the substrate and CrYN:Nb doped films were found as 316L:2253.5, MC-1:2393.4, MC-2:2492.4, MC-3:2659.9, respectively (Figure 11a and Table 2). All coated samples showed a higher bending moment compared to the substrate. While the bending stress/strength ( $\sigma$ e, MPa) was 602.2 for the substrate, it was found as 684.9

for MC-1, 664.7 for MC-2, 707 for MC-3. An increase in bending strength is observed in all coated samples (Figure 12). The values of the modulus of elasticity (E) were obtained as 173.9 for the substrate, 183.7 for MC-1, 180.4 for MC-2, 190.9 for MC-3 (Table 2). Similar to all other data, an increase in the modulus of elasticity was observed in the coated samples compared to the substrate. It is thought that the increases in the bending moment, bending strength and elasticity modulus compared to the uncoated substrate indicate an increase in strength. In the Nb-doped films, the highest bending strength was shown in the experiments by MC-3 (707 MPa) (Fig. 12). The highest hardness was also found in the MC-3 experiment in terms of hardness values (Fig. 4d). This indicates that the hardest coating has the highest bending strength and an increase in strength. Similarly, the highest values in bending moment and elasticity modulus were observed in the MC-3 experiment. When the coating thicknesses were evaluated, it was found that the MC-3 coating was the thickest film (2.8 μm) and had a dense/smooth microstructure. Sample MC-3 is the thickest (2.8 µm), the hardest (21.4 GPa), the second highest corrosion resistance (12.3 nA) and the highest bending strength (707 MPa) [19]. Analysis of the experimental parameters determined in this study shows that the film (MC-3) has the most optimum conditions among the Nb-doped films (Fig. 12).

260

261

262

263

264

265

266

267

268

269

270

271

272

273

274

275

276

277

278

279

280

281

282

283

284

285

286

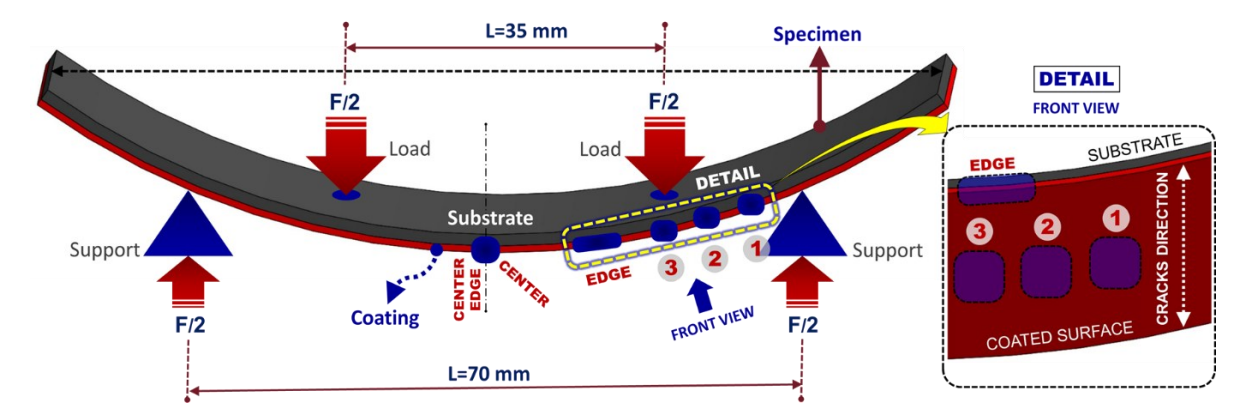
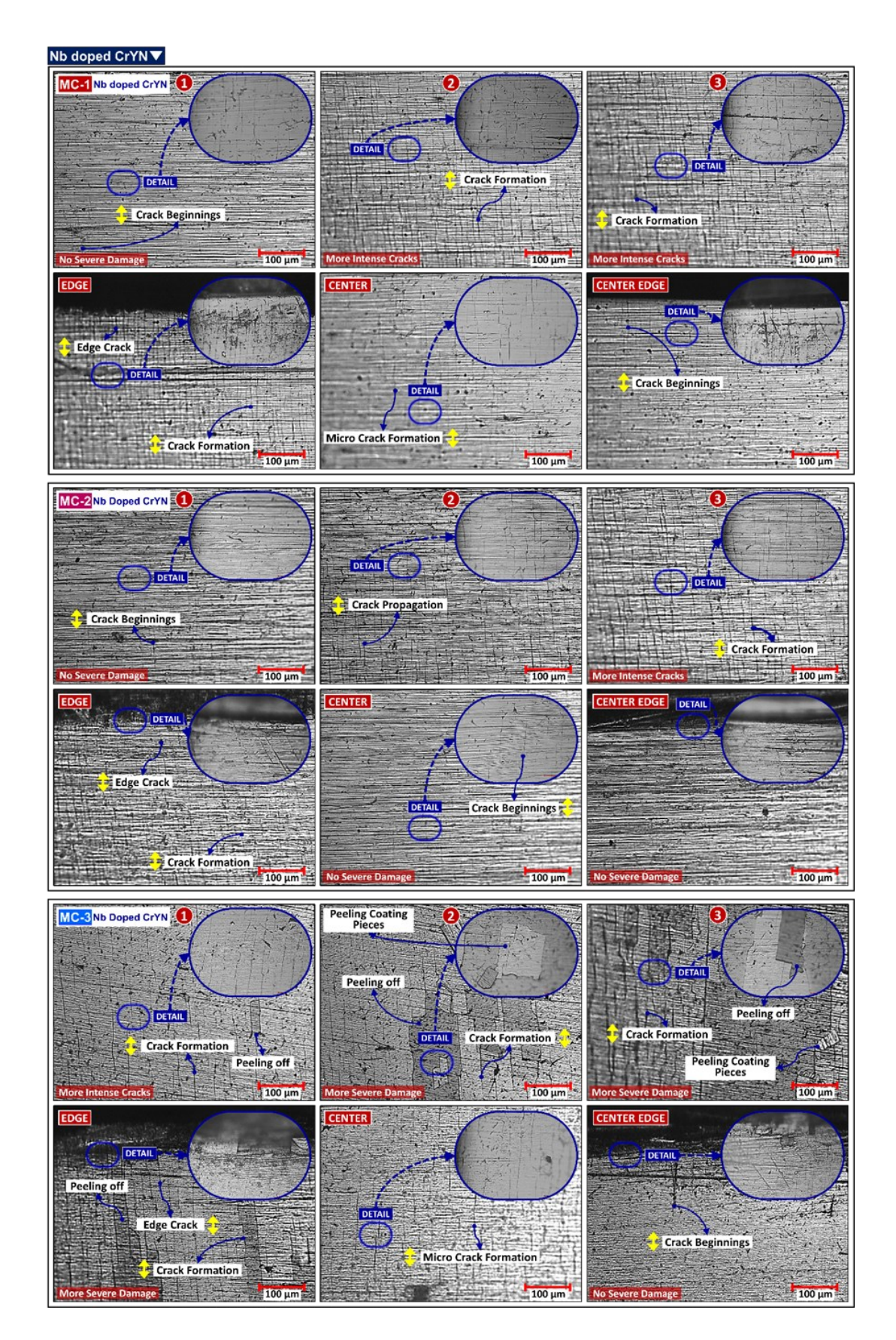


Fig. 13. The representative shape of the outer bending surfaces of specimens subjected to 4-point bending test

It is thought that increases in bending moment, bending strength and elasticity modulus indicate an increase in strength. In Ta-doped films, the highest bending strength among the samples was shown by the MC-3 (711.3 MPa) sample (Figure 12). The highest hardness values were also observed in MC-2 and MC-3 samples. This indicates that the hardest coatings have the highest bending strength and an increase in strength. Similarly, the highest values in bending moment and elasticity modulus values were observed in the MC-3 sample. Similar to the Nb-doped films, the MC-3 sample has the highest thickness (2.26 µm) in Ta-doped films and has a very dense/smooth microstructure. This shows us that there is a positive correlation between

thickness, hardness and bending strength. There are also studies in the literature that both doping elements improve the mechanical properties of thin films [7-11]. In our study, an increase in the bending strength was observed in all experiments from MC-1 to MC-3 with both doping elements, and the literature data is consistent with our study. The variable parameters determined in the experimental design are CrY target current (1, 1.5, 2A), working pressure (0.15, 0.25, 0.35 Pa), pulse frequency (100 kHz) and duty cycle (50%, 70%, 85%). As the target current increases, the amount of sputtered target atoms increases. This results in an increase in the amount of deposition [25-26]. In accordance with the literature, in our study, the thickest, hardest and highest bending strength films were synthesized in the experiment with the lowest pulse frequency (100 kHz) and the highest target current (2A) for both Nb, Ta and V [18-19].



**Fig. 14.** 4-point bending optical microscope images of Nb-doped CrYN coatings (MC-1, MC-2 and MC-3)

For all coating samples, optical microscope images were taken from the sections indicated in the image in Figure 13 and evaluations were made about the damage mechanisms. Micro crack formation, crack initiation, crack propagation and edge cracks are observed in MC-1 and MC-2 coatings. In MC-1 and MC-2, crack densities in the 3rd region and the center are quite close to each other. When the detailed images are examined, there is more intense crack formation in the center, edge and edge regions. This can be attributed to the stress concentrations occurring at the edges. In MC-3 coating, it was observed that crack formation was quite intense in the 1st region and the presence of areas where the coating was separated. In the 2nd region, there are areas where the coating was separated and broken coating pieces. In the 3rd region, that is, the section where the crack density is the highest, deep crack formations, coating separation in a larger area and broken coating pieces were observed that were not present in other coatings. There are more intense crack formation and edge cracks in the center and center edge of MC-3 coating compared to other coatings. In the edge region, frequent crack formation and areas where the coating was separated were observed. MC-3 coating was found to be both the hardest (21.4 GPa) and the coating with the highest bending strength (707 MPa) in the 4-point bending and hardness test. Sample MC-3 is also the film with the highest thickness (2.8 µm). The inverse relationship between thickness and adhesion can also explain the current situation (as the thickness increases, the amount of internal stress in the coating increases). In the 4-point bending tests, it can be said that the coating is lifted off the surface in the final state, which occurs when crack formation and growing cracks reach or do not reach the edge. These damages can be attributed to the hardness, hence the film being more brittle and the lower adhesion. Among the CrYN:Nb coatings, the highest crack density and coating separation regions were observed in MC-3, which is the hardest and has the highest bending strength. In the detailed images of all films, crack formation, crack density, film separation and rupture (due to the effect of low adhesion) are given in the relevant images (MC-1-MC-3 Details).

300

301

302

303

304

305

306

307

308

309

310

311

312

313

314

315

316

317

318

319

320

321

322

323

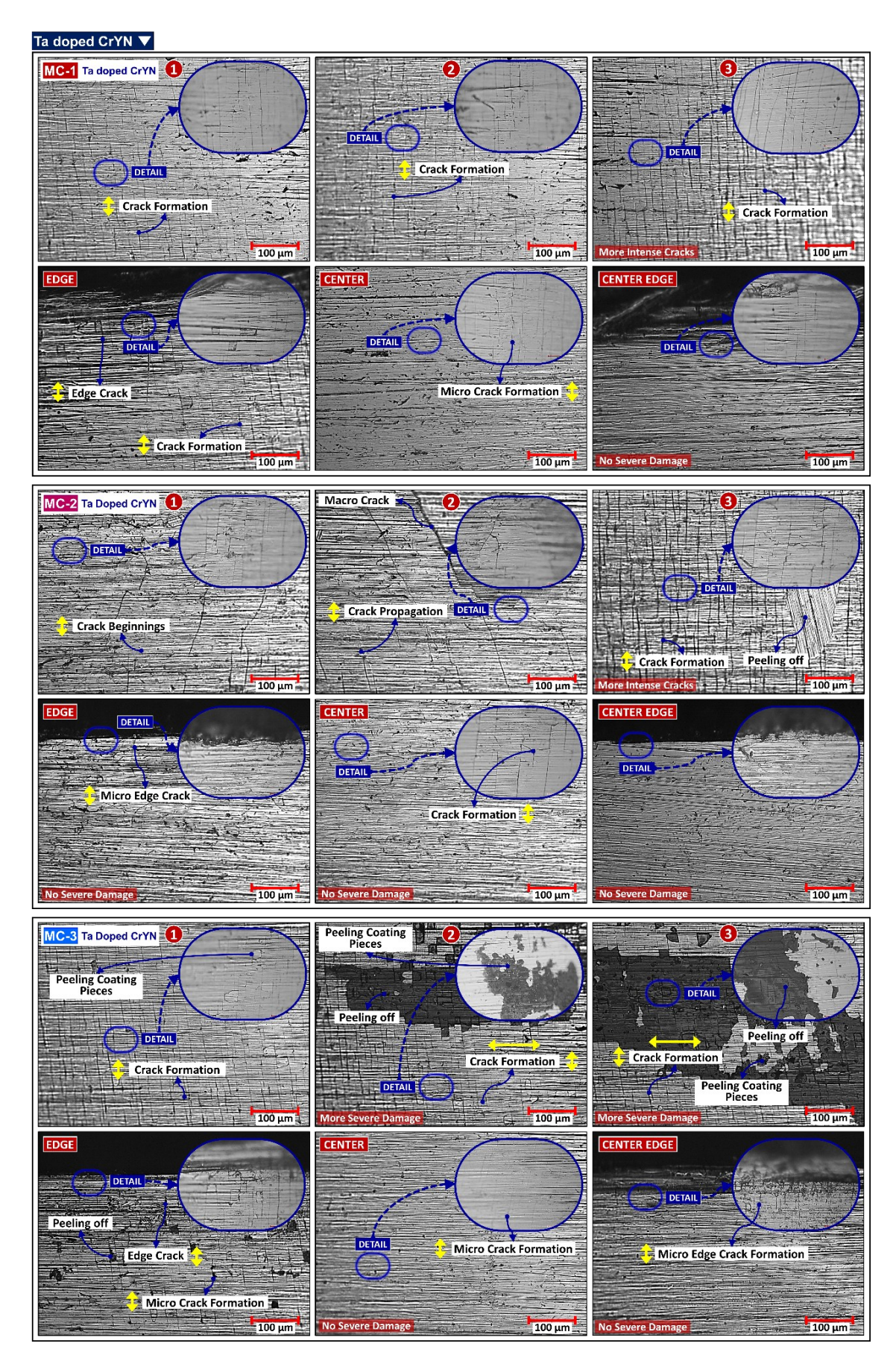


**Fig. 15.** 4-point bending optical microscope images of Ta-doped CrYN coatings (MC-1, MC-2 and MC-3)

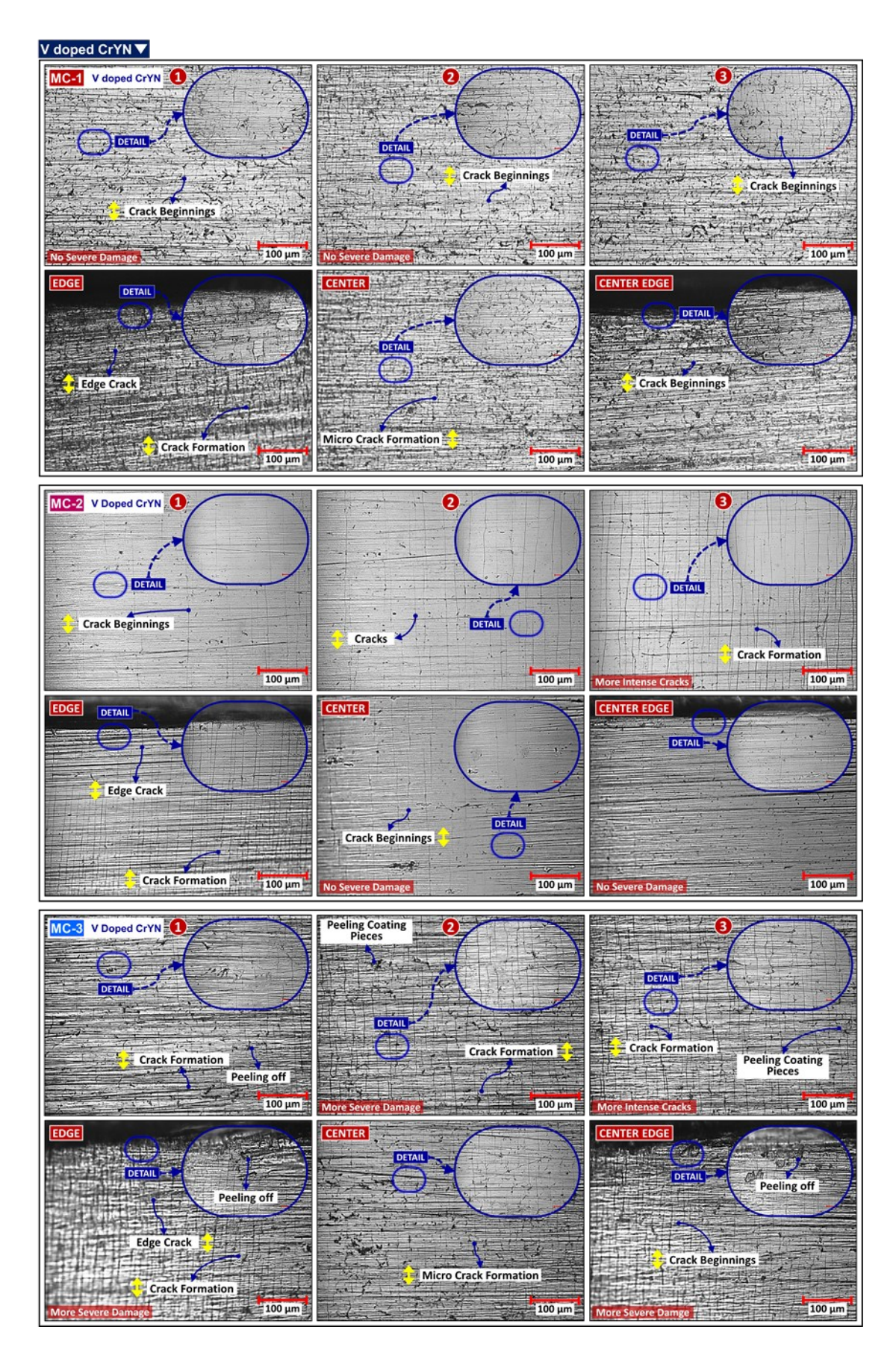


**Fig. 16.** 4-point bending optical microscope images of Ta-doped CrYN coatings (MC-1, MC-2 and MC-3)

In the MC-1 coating, there are crack initiations in the first region, more increasing crack propagation in the second region, and dense and frequent cracks in the third region. While there is no crack formation in the central region, there are edge damages at the central edge. In the edge part of the third region, there are quite dense edge cracks and coating flaking (indicating low adhesion). It is thought that this is caused by stress concentrations in the edge regions. In addition to these, the coating MC-1 coating has a hardness of 15.1 GPa and a bending stress of 676 MPa. The MC-2 coating has the highest hardness (18.2 GPa) and quite high bending strength (675 MPa) among Ta-doped films. In this coating, there are deep crack formations and flaking in the first region, particles from which the coating has separated in the second region, and broken coating pieces in the third region, deep and frequent crack formations. While there are no cracks in the center and central edge, there is microcrack formation at the edge since the stress amount is more intense at the edge of the 3rd region. In MC-3, crack formation, flaking and peeling are observed in the first region, coating peeling and peeling in the form of large particles in the second region, and an increase is observed in the area where the coating peels off in the third region. Although damage formation is quite low in the center and center edge, there are peeling, flaking and edge cracks (due to stress concentrations) at the edge. MC-3 coating is the coating with the highest bending strength (CrYN:Nb/Ta/V-707/711/709 MPa) in both Nb, Ta and V doped films. In addition, since the hardness value (15 GPa) is quite high compared to other Ta coated samples (among the three hardest coatings), damages in the coating were greater. At the same time, MC-3 film has the highest thickness among Ta doped films. The inverse relationship between thickness and adhesion can also explain the current situation. In the 4-point bending tests, it can be said that the coating is removed from the surface in the final situation, which occurs when crack formation and growing cracks reach or do not reach the edge. These damages can be attributed to the hardness, hence the film being more brittle and the lower adhesion. It is observed that crack initiations in the second region, and crack propagation in the third region and edge are increased compared to the second region (Figure 14-16). As the hardness decreases, the bending strength also decreases. The results show that films with lower hardness are more ductile and have less damage to the coating. In the 4-point bending tests, it can be said that the coating is lifted off the surface in the final state, when crack formation and growing cracks reach or do not reach the edge. These damages can be attributed to the hardness, therefore the film being more brittle and the adhesion being lower. At the same time, the most coating damage is present in the thickest films. This can be explained by the inverse relationship between adhesion and thickness (internal stresses in the structure increase as the thickness increases). The damage that occurs more at the edge and center edges

331

332

333

334

335

336

337

338

339

340

341

342

343

344345

346

347

348

349

350

351

352

353

354

355

356

357

358

359

360

361

362

363

indicates the stress concentrations accumulated in these regions. In both coating types, the maximum crack formation occurred approximately between the second and third regions (closer to approximately three). This can be attributed to the shear force diagram of the 4-point bending test. Similar results have been observed in similar studies [27-32]. Both coatings exhibited higher bending strength (substrate: 602 MPa, Nb-CrYN MC-3: 707 MPa, Ta-CrYN MC-3: 711 MPa and V-CrYN:709.7 MPa) and bending moment (substrate: 2253 Nmm MPa, Nb-CrYN MC-3: 2659 Nmm, Ta-CrYN MC-3: 2598 Nmm, V-CrYN:2663.1 Nmm) values compared to the substrate. Less coating damage was observed in Nb-doped films compared to Ta-doped films in optical microscope examinations. Considering that the only difference between the two coating types is the additive elements, the positive effect of niobium on mechanical properties is greater than that of tantalum. This is consistent with the existing literature [6-10]. Specifically, the hardness and adhesion behaviors obtained from the nanoindentation and scratch tests have been linked to the coating performance in tribological and protective applications. The observed hardness values of 21.4 GPa, 18.2 GPa, and 16.1 GPa for Nb-, Ta-, and V-doped CrYN films, respectively, indicate that Nb addition significantly enhances film densification and cohesive strength through solid-solution and grain refinement mechanisms. This improved hardness is technologically relevant for wear-resistant coatings, particularly in cutting or forming tools operating under high load conditions. Similarly, the scratch test results demonstrate that Nb-, Ta-, and V-doped CrYN coatings maintain good adhesion to the substrate, with the most pronounced damage occurring in MC-3 samples, consistent with four-point bending test results. The strong correlation between adhesion strength and bending resistance implies that dopant type and process conditions directly affect the coating-substrate interface integrity. Among the dopants, V provided the best adhesion performance, indicating its suitability for applications requiring high toughness and reduced delamination risk, such as high-speed machining and thermal barrier layers. These correlations confirm that the microstructural and mechanical responses observed experimentally have direct technological implications for optimizing coating design toward enhanced durability, adhesion, and performance under mechanical stress.

#### 4. Conclusions

365

366

367

368

369

370

371

372

373

374

375

376

377

378

379

380

381

382

383

384

385

386

387

388

389

390

391

392

393

394

395

In this study, the mechanical, structural and chemical properties of Nb, Ta and V doped CrYN thin films grown on 316L SS substrate were investigated.

XPS spectra were performed for CrYN:Nb/Ta/V thin films. For Nb, Ta and V doped thin films, scans were performed at Cr 2p, Y 3d and N 1s. In addition, the corresponding peaks were obtained at Nb 3d for niobium, Ta 4d for tantalum and V 2p for vanadium.

- ✓ Maximum nanohardness results for CrYN:Nb/Ta/V were determined as 21.4 GPa, 18.2 GPa, 16.1 GPa respectively. The most effective parameter affecting hardness in both films is the pulse frequency.
- ✓ When the XRD peaks of CrYN:Nb/Ta/V thin films and the substrate are analyzed, there are intense cubic CrN and Cr₂N peaks except for the main peaks coming from the substrate. NbN, TaN and VN peaks were obtained in niobium/tantalum and vanadium doped thin films, respectively. Yttrium is thought to be present in the structure as a substitutional atom of chromium.
- ✓ When coating thicknesses and microstructure were examined, a dense and homogeneous structure was obtained in all three (CrYN:Nb/Ta/V) composite thin films. The highest film thickness for niobium was observed in MC-3 at 2.80 μm. Similar to the niobium doped film, the highest film thickness in the tantalum doped coating was found to be 2.26 μm at MC-3 (Duty cycle 85 %, deposition pressure 0.35 Pa, CrY target current 2 A). The influence of the magnetron sputtered-Pulsed DC power supply on the dense and uniform film structure cannot be ignored.
- ✓ The scratch test results of Nb/Ta/V doped CrYN films showed micro cracks, edge cracks, buckling, peeling and chipping damage. For all doped films, the most damage occurred in MC-3 film. When the three doping elements were evaluated, the least damage was observed in V-doped CrYN films. This shows similar results to the results of the four bending tests.
- ✓ In the four-point bending test results, an increase in the maximum force (Fmax), bending moments, bending strengths and elasticity modules applied to all CrYN:Nb/Ta/V films compared to the substrate is observed. In Nb-doped films, the highest bending strength among the samples was shown by the MC-3 (707 MPa) test. In Ta-V doped films, the highest bending strength among the samples was shown by the MC-3 (711.3 MPa, 709.7 MPa) test. In our study, it was observed that both additive elements provided an increase in bending strength in all the tests conducted from MC-1 to MC-3, and the literature information is consistent with our study. It was found that the bending strengths of the films with high hardness were also high. This may indicate a correlation between bending strength and hardness. Increases in bending moment, bending strength and elasticity module indicate an increase in strength.

✓ When the optical microscope images taken from several different regions of the bending points (external bending surfaces) of all coated samples subjected to the four-point bending test were examined, the highest crack formation, flaking, parts breaking off from the coating and damage formation were observed in the MC-3 test in both CrYN:Nb/Ta/V thin films. The MC-3 coating has the highest bending strength in both film types. In addition to these, it is seen that there is more crack formation and coating damage in films with high hardness. It is clear that the adhesion strength of the MC-3 film is lower than the other films. In addition, the MC-3 film has a high thickness. This can be explained by the relatively inverse relationship between adhesion and thickness. Damage/delamination was observed more in films that are thought to be more brittle than the others.

In summary, among the additives examined, the addition of Nb provided the highest hardness and mechanical strength for CrYN coatings, while the addition of V provided superior adhesion and resistance to cracking and delamination. Ta, on the other hand, showed moderate performance. Therefore, Nb can be considered the most suitable additive for applications requiring maximum hardness and wear resistance, while V is considered more suitable for applications requiring advanced adhesion and toughness.

# **CRediT** authorship contribution statement

# **Declaration of competing interest**

- The authors declare that they have no known competing financial interests or personal relationships that could have appeared to influence the work reported in this paper.
  - Data availability
- Data will be made available on request.

#### Acknowledgements

- This research was supported by Royal Society Projects (Grant Agreement No: IES\R2\202084)
- and Atatürk University-BAP (Grant Agreement No: FDA-2022-11399). The authors would
- like to thank to Royal Society and Atatürk University for funding the project.

# References

[1] X. Li, W. Wu, H. Dong, Microstructural characterisation of carbon doped CrAlTiN nanoscale multilayer coatings, Surf Coat Technol. 205 (2011) 3251–3259, https://doi.org/10.1016/J.SURFCOAT.2010.11.046.

[2] Y.I. Chen, K.Y. Lin, C.C. Chou, Thermal stability of CrTaN hard coatings prepared using biased direct current sputter deposition, Thin Solid Films 544 (2013) 606–611, https://doi.org/10.1016/J.TSF.2012.11.047.

[3] A. Keles, H. Çiçek, "O. Baran, Y. Totik, I. Efeoglu, Determining the critical loads of V and Nb doped ternary TiN-based coatings deposited using CFUBMS on steels, Surf. Coat. Technol. 332 (2017) 168–173, https://doi.org/10.1016/J. SURFCOAT.2017.07.085.

[4] Y. Ren, J. Jia, X. Cao, G. Zhang, Q. Ding, Effect of ag contents on the microstructure and tribological behaviors of NbN–ag coatings at elevated temperatures, Vacuum 204 (2022), 111330, https://doi.org/10.1016/J.VACUUM.2022.111330.

[5] M.M. Al-Asadi, H.A. Al-Tameemi, A review of tribological properties and deposition methods for selected hard protective coatings, Tribol Int. 176 (2022), 107919, https://doi.org/10.1016/J.TRIBOINT.2022.107919.

[6] P.E. Hovsepian, A.P. Ehiasarian, Y.P. Purandare, P. Mayr, K.G. Abstoss, M. M. Feijoo, J.P. Trujillo, Novel HIPIMS deposited nanostructured CrN/NbN coatings for environmental protection of steam turbine components, J. Alloys Compd. 746 (2018) 583–593, <a href="https://doi.org/10.1016/j.jallcom.2018.02.312">https://doi.org/10.1016/j.jallcom.2018.02.312</a>.

[7] S.B. Hung, C.F. Wang, Y.Y. Chen, J.W. Lee, C.L. Li, Thermal and corrosion properties of V-Nb-Mo-Ta-W and V-Nb-Mo-Ta-W-Cr-B high entropy alloy coatings, Surf. Coat. Technol. 375 (2019) 802–809, https://doi.org/10.1016/j. surfcoat.2019.07.079.

[8] Z.T. Wu, Z.B. Qi, D.F. Zhang, B.B. Wei, Z.C. Wang, Evaluating the influence of adding Nb on microstructure, hardness and oxidation resistance of CrN coating, Surf. Coat. Technol. 289 (2016) 45–51, https://doi.org/10.1016/j. surfcoat.2016.01.047.

[9] B. Trindade, W.Z. Li, F. Fernandes, A. Cavaleiro, Effect of Nb target power on the structure, mechanical properties, thermal stability and oxidation resistance of Cr–Al–Nb–N coatings, Surf. Coat. Technol. 285 (2016) 270–277, https://doi.org/10.1016/j.surfcoat.2015.12.002.

[10] D. Wang, Y. Fu, M. Hu, D. Jiang, X. Gao, Q. Wang, L. Weng, Effect of Nb content on the microstructure and corrosion resistance of the sputtered Cr-Nb-N coatings, J. Alloys Compd. 740 (2018) 510–518, https://doi.org/10.1016/j.jallcom.2018.01.034.

[11] P. Hones, R. Sanjin'es, F. L'evy, Sputter deposited chromium nitride based ternary compounds for hard coatings, Thin Solid Films 332 (1998) 240–246, https://doi. org/10.1016/S0040-6090(98)00992-4.

[12] B. Liu, B. Deng, Y. Tao, Influence of niobium ion implantation on the microstructure,
 mechanical and tribological properties of TiAlN/CrN nano-multilayer coatings, Surf Coat
 Technol. 240 (2014) 405–412, https://doi.org/10.1016/J.SURFCOAT.2013.12.065.

- [13] Zhao, J., Xu, Y., & Ding, X. (2022). An in-depth understanding of the solvation effect of methanol on the anisotropy of electrochemical corrosion of Ta. *Electrochimica Acta*, 435, 141359. <a href="https://doi.org/10.1016/j.matlet.2015.10.091">https://doi.org/10.1016/j.matlet.2015.10.091</a>.
- [14] Kainz, C., Kölbl, L., & Schalk, N. (2022). On the influence of the Cr/(Cr+ Ta) ratio on the microstructure, mechanical properties and thermal stability of magnetron sputtered CrxTa1-xN coatings. *Surface and Coatings Technology*, 447, 128877. <a href="https://doi.org/10.1016/j.surfcoat.2022.128877">https://doi.org/10.1016/j.surfcoat.2022.128877</a>
  - [15] Jang, Y., Kim, Y., Jeong, W., Ko, S., Gil, D., Jeong, I., ... & Cha, S. W. (2024). Corrosion behavior of Ta and TiN double-layer-coated SUS316L for PEMFC bipolar plates using plasma-enhanced atomic layer deposition and magnetron sputtering. *Journal of Alloys and Compounds*, 977, 173379. https://doi.org/10.1016/j.jallcom.2023.173379
- [16] Hu, C., Zhang, J., Liu, H. J., Du, J. W., Chen, L., Kong, Y., & Mayrhofer, P. H. (2024).
   Ab initio supported development of Nb-and Ta-alloyed (Ti, Al) N thin films with improved thermal stability. Surface and Coatings Technology, 483, 130763.
   <a href="https://doi.org/10.1016/j.surfcoat.2024.130763">https://doi.org/10.1016/j.surfcoat.2024.130763</a>
  - [17] Rapoport, L., Moshkovich, A., Perfilyev, V., Lapsker, I., Kugler, M., Kailer, A., ... & Hollstein, T. (2014). High temperature friction behavior of CrVxN coatings. *Surface and Coatings Technology*, 238, 207-215. <a href="https://doi.org/10.1016/j.surfcoat.2013.10.076">https://doi.org/10.1016/j.surfcoat.2013.10.076</a>
  - [18] Gulten, G., Yaylali, B., Efeoglu, I., Totik, Y., Kelly, P., & Kulczyk-Malecka, J. (2024). Effect of Nb and V doped elements on the mechanical and tribological properties of CrYN coatings. Surface and Coatings Technology, 477, 130297.
  - [19] Yaylali, B., Gulten, G., Efeoglu, I., Totik, Y., Kelly, P., & Kulczyk-Malecka, J. (2024). Influence of Nb and Ta on the corrosion and mechanical properties of CrYN coatings. Surface and Coatings Technology, 476, 130249.
    - [20] A. Keles, H. Çiçek, "O. Baran, Y. Totik, 'I. Efeo glu, Determining the critical loads of V and Nb doped ternary TiN-based coatings deposited using CFUBMS on steels, Surf. Coat. Technol. 332 (2017) 168–173, https://doi.org/10.1016/j. surfcoat.2017.07.085.
    - [21] S. Liu, B. De Ong, J. Guo, E. Liu, X. Zeng, X, Wear performance of Y-doped nanolayered CrN/AlN coatings, Surf. Coat. Technol. 367 (2019) 349–357, https://doi.org/10.1016/j.surfcoat.2019.02.092.
- [22] Z.B. Qi, Z.T. Wu, Z.C. Wang, Improved hardness and oxidation resistance for CrAlN hard coatings with Y addition by magnetron co-sputtering, Surf. Coat. Technol. 259 (2014)
   146–151, <a href="https://doi.org/10.1016/j.surfcoat.2014.02.034">https://doi.org/10.1016/j.surfcoat.2014.02.034</a>.

- [23] M.T. Myandoab, CrAlYN/CrY Multilayer Composite Thin Film Synthesis: Structural-554
- Mechanical-Tribological and Thermal Properties of Investigation, Institute of science. 555
- (PhD Ataturk university. 2016 Thesis), https://tez.yok.gov.tr/ 556
- UlusalTezMerkezi/tezDetay.jsp?id=y9uRDDYo9nldTmxEMvmqSQ&no=NLA 557
- GBO16bic0vTM2WdfXUQ. 558

[24] Wu, Z. T., Qi, Z. B., Zhang, D. F., & Wang, Z. C. (2016). Nanoindentation induced 560 plastic deformation in nanocrystalline ZrN coating. Materials Letters, 164, 120-123. 561 https://doi.org/10.1016/j.matlet.2015.10.091 562

563

[25] Zhang, Y., Song, Q., & Sun, Z. (2012). Research on thin film thickness uniformity for 564 deposition of rectangular planar sputtering target. Physics Procedia, 32, 903-913. BY-565 7325-Taslak-ICMCTF-Abstract-Analysis of Four-Point Bending Test for Nb, Ta, and V-566 Doped CrYN Thin Films Deposited by Closed-Field Unbalanced Magnetron 567 Sputtering.docx 568

569

[26] Huang, P. C., Huang, C. H., Lin, M. Y., Chou, C. Y., Hsu, C. Y., & Kuo, C. G. (2013). 570 The effect of sputtering parameters on the film properties of molybdenum back contact for 571 CIGS cells. International Journal Photoenergy, 2013(1), 390824. 572 solar of https://doi.org/10.1155/2013/390824 573

574

[27] Leonhardt, F., & Walther, R., 1963. Shear Tests on T-Beam with Varying Shear 575 Reinforcement. Deutscher Ausschuss für Stahlbeton, (156), 84. 576

577

[28] Chu, J. P., Greene, J. E., Jang, J. S., Huang, J. C., Shen, Y. L., Liaw, P. K., ... & 578 Nieh, T. G. (2012). Bendable bulk metallic glass: Effects of a thin, adhesive, strong, and 579 ductile coating. Acta Materialia, 60(6-7), 3226-3238. 580 https://doi.org/10.1016/j.actamat.2012.02.037

581

582

[29] Tesárek, P., Trejbal, J., Topič, J., Prošek, Z., Nežerka, V., & Lidmila, M. (2016). 583 Effect of Reinforcement on Flexural Strength and Ductility of Gypsum-Based 584 585 Composites with Recycled Wires from Automobile Tires. Applied Mechanics and Materials, 827, 348-351. https://doi.org/10.4028/www.scientific.net/AMM.827.348 586

587 588

589

590

[30] Jiang, P., Fan, X., Sun, Y., Li, D., & Wang, T. (2018). Bending-driven failure mechanism and modelling of double-ceramic-layer thermal barrier coating system. International Journal Structures, 130, 11-20. Solids and https://doi.org/10.1016/j.ijsolstr.2017.10.024

591 592 593

594

595

[31] He, J., Xie, D., Xue, Q., & Zhan, Y. (2018). Seawater effects on static loads and interlayer cracking performance for polyvinyl chloride foam-cored sandwich Engineering, 10(11), 1687814018807342. composites. Advances in Mechanical https://doi.org/10.1177/1687814018807342

596 597 598

599

[32] Alasadi, S., Ibrahim, Z., Shafigh, P., Javanmardi, A., & Nouri, K. (2019). An experimental and numerical study on the flexural performance of over-reinforced concrete beam strengthening with bolted-compression steel plates: Part II. Applied Sciences, 10(1),

601 94. <a href="https://doi.org/10.3390/app10010094">https://doi.org/10.3390/app10010094</a>